Learning approach to analyze tumour heterogeneity in DCE-MRI data during anti-cancer treatment

A. Daducci[2], U. Castellani[1], M. Cristani[1], P. Farace[2], P. Marzola[2], A. Sbarbati[2], V. Murino[1]

[1] VIPS lab, University of Verona, Italy
[2] Department of Morphological-Biomedical Sciences, Section of Anatomy and Histology, University of Verona, Italy

Abstract. The paper proposes a learning approach to support medical researchers in the context of in-vivo cancer imaging, and specifically in the analysis of Dynamic Contrast-Enhanced MRI (DCE-MRI) data. DCE-MRI techniques are applied to monitor the development of the tumour micro-vessels. Tumour heterogeneity is characterized by identifying regions with different vascular perfusion. The overall aim is to measure volume differences of such regions for two experimental groups: the treated group, to which an anticancer therapy is administered, and a control group. In this way a non-invasive method for the analysis of the treatment efficacy is obtained. The proposed approach is based on a three-steps procedure: (i) robust features extraction from raw time-intensity curves, (ii) sample-regions identification manually traced by medical researchers on a small portion of input data, and (iii) overall segmentation by training a Support Vector Machine (SVM) to classify the MRI voxels according to the previously identified cancer areas. In particular, after this phases the SVM is able to classify unseen subjects with the same kind of tumour. Results obtained in the present work report convincing analysis of tumour heterogeneity by allowing quantitative measurements of volumetric changes within the identified tumoral regions. The evaluation of such differences between the two experimental groups, is useful for an efficacy study of the anticancer therapies.

1 Introduction

In the context of cancer imaging, machine learning techniques are becoming important to automatically isolate areas of interest characterized by heterogeneous tumoural tissues. In particular, the identification of tumour heterogeneity is crucial for diagnosis and therapy assessment. In this paper, tumour morphology and functional perfusion are obtained by Dynamic Contrast Enhanced MRI (DCE-MRI) techniques. We propose a learning-by-example approach[1] to classify tumoral regions characterized by heterogeneous vascular perfusion. In fact, DCE-MRI techniques represent noninvasive ways to assess tumour vasculature,

that are accepted surrogate markers of tumour angiogenesis [2]. Data are analyzed with the aim of investigating the volume changes in the identified regions for both untreated and treated tumours. As a result, a method for in-vivo evaluation of treatment efficacy becomes available to assess anticancer therapies.
The proposed analysis is based on three main phases: (i) features extraction from raw time-intensity curves, (ii) representative tumour areas identification, and (iii) overall voxel-by-voxel classification. In the first phase, few robust features that compactly represent the response of the tissue to the DCE-MRI analysis are computed. The second step provides a manual identification of tumour samples that are representative of the typical tumour aspects. Such samples are carefully and manually chosen by a medical researcher on a small portion of input data by observing the different behavior of the time-intensity signals within different kind of tumoural regions (i.e., necrotic or still alive zones). Finally, in the third step, a Support Vector Machine (SVM) is trained to classify voxels according to the regions (i.e., typologies of tumour tissue) defined by the previous phase. In this way, the SVM is able to automatically detect the most discriminative characteristics of the manually identified regions by extending such capability to classify unseen subjects.

Several works are based on the use of machine learning techniques for DCE-MRI tumour analysis [3–6]. In [3], a visual data-mining approach is proposed to support the medical researchers in tumoral areas characterization by clustering data according to the transendothelial permeability (kPS) and fractional plasma volume (fPV). Although kPS and fPV are accepted estimate of tissue vasculature, it is proved their instability under small perturbation of the chosen pharmacokinetics model [4, 5]. Therefore, different works are addressed the idea of analyzing directly the raw signals by exploiting possible other compact parameters of the curve shapes. As an example, in [4] the raw signals of the DCE-MRI voxels are analyzed in the context of musculoskeletal tissue classification. Several features are extracted to represent the signals shape such as the maximum signal intensity, the largest positive signal difference between two consecutive scans, and so on. Then, the classification is carried out by introducing a thresholding approach. In [5] the authors propose the use of the Mean Shift algorithm [7] for the clustering of breast DCE-MRI lesions. In particular, voxels are clustered according to the area under the curve feature. Since the results are over-segmented, an iterative procedure is introduced to automatically select the clusters which better represent the tumour. Similarly, in our previous work [8], tumoral regions are characterized by combining Mean Shift clustering[7] with Support Vector Machine (SVM) classification. In [6] a learning-by-example approach is introduced to detect suspicious lesions in DCE-MRI data. The tumoural pixels are selected in a supervised fashion and fed to a SVM which is trained to perform a binary classification between healthy and malignant pixels. The raw n-dimensional signal is used as multidimensional vector.

In the present work we extend the basic framework proposed in [8], to asses the treatment efficacy of anticancer therapies. The above described analysis is applied on two groups of animals (treated and control) at two time points (i.e.,

T_0 and T_1). At the end of the treatment period (time point T_1) the differences in tumour evolutions between the two groups were assessed by measuring volumetric differences on the various detected regions. The rest of the paper is organized as following. Section 2 introduces the experimental design and data acquisition process. Section 3 describes the proposed method by detailing the main phases involved on the proposed framework. Exhaustive results are shown and discussed in Section 4, and finally conclusions are drawn in Section 5.

2 Materials

2.1 Experimental design

Tumours were induced by subcutaneous injection of human carcinoma cells in nude mice ($n = 11$). Ten days after cells injection animals were randomly assigned to the treated ($n = 6$) and control group ($n = 5$). Animals belonging to the treated and control group received an experimental drug and vehicle, respectively, for a period of 7 days. All animals were observed by MRI before (time T_0) and after the treatment (time T_1). A further group of mice ($n = 5$) bearing the same kind of tumour was used in the training step of the classification procedure.

2.2 Data acquisition

Animals were examined using DCE-MRI with *MS-325* (*Vasovist®, Schering Germany*) as contrast agent. Mice were anesthetized by inhalation of a mixture of air and O_2 containing $0.5-1\%$ isofluorane, and placed in a prone position inside a 3.5 cm i.d. transmitter-receiver birdcage coil. Images were acquired using a Biospec tomograph (*Bruker, Karlsruhe, Germany*) equipped with a 4.7 T, 33 cm bore horizontal magnet (*Oxford Ltd., Oxford, UK*). DCE-MRI experiments were performed as previously described [2, 9, 10]. Briefly, after tumour localization, a dynamic series of transversal spoiled-gradient echo (SPGR) 3D images were acquired with the following parameters: repetition time/echo time 50/3.5 ms, flip angle (90°), matrix size $256\times128\times16$, field-of-view $6\times3\times2.4$ cm^3 (corresponding to 0.234×0.234 mm^2 in-plane resolution and 1.5 mm slice thickness), number of acquisitions = 1. The acquisition time for a single 3D image was 102 seconds; dynamic scans of 25 images were acquired at 5-second intervals (total acquisition time approximately 45 minutes). The contrast agent was injected in bolus during the time interval between the first and the second scan at 100 $\mu mol/kg$ dosage.

3 Proposed Method

At each time point, signal intensity values have been normalized to the pre-contrast value and filtered using a smoothing function to minimize fluctuations due to movement artefacts or noise. To account for tumour heterogeneity, seven classes have been fixed by combining a-priori knowledge of medical experts with the observation of signal shape behaviors (see `A-G` in Figure 1):

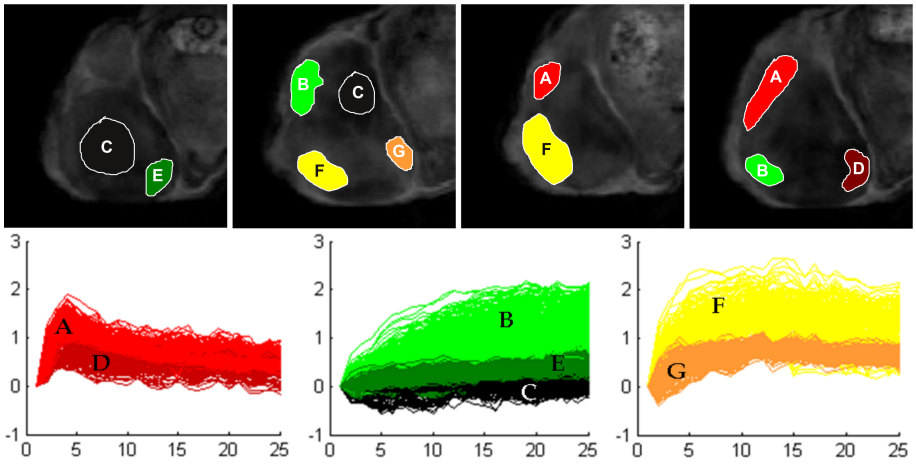

Fig. 1. Sample regions used for SVM training. To account for tumour heterogeneity seven classes (`A-G`) were chosen by a-priori knowledge. Source data used to select the sample regions (TOP), and the relative DCE-MRI curves of the whole training set are reported (BOTTOM).

- **Classes `A` and `D`**, are characterized by contrast agent wash-out (i.e., clear defined peak followed by a decrease). These regions correspond to highly vascularized and viable tumor tissue. Regions `A` and `D` differ by the value of maximum intensity.
- **Classes `B` and `E`**, reveal contrast agent accumulation (i.e., increasing trend). Presumably, this areas correspond to viable tissue with reduced vascularization, evidencing the transition of the tumor toward a necrotic state. Again, regions `B` and `E` differs by the value of maximum intensity.
- **Class `C`**, contains voxels with negligible enhancement, typically due to necrotic and not vascularized tissue.
- **Classes `F` and `G`**, have been introduced to account for intermediate patterns (i.e., initial increasing trend followed by a plateau phase).

By following the proposed pipeline, few and stable signal features are identified to model the different DCE-MRI curve classes. In particular the following curve characteristics are chosen: time-to-peak (TTP), peak value ($PEAK$), area under curve (AUC), initial area under curve (AUC_{TTP}), and wash-out rate (WR) (see Figure 2). Therefore, in order to apply a learning-by-example approach, several samples of each identified class need to be fed to the classifier. As mentioned above, such phase is carried out manually by medical experts. Figure 1(TOP) shows some representative regions which are used to build the training set. In Figure 1(BOTTOM) the signals curve of the whole selected samples are reported. Signals are colored according to their respective class by evidencing the expected curve shape.

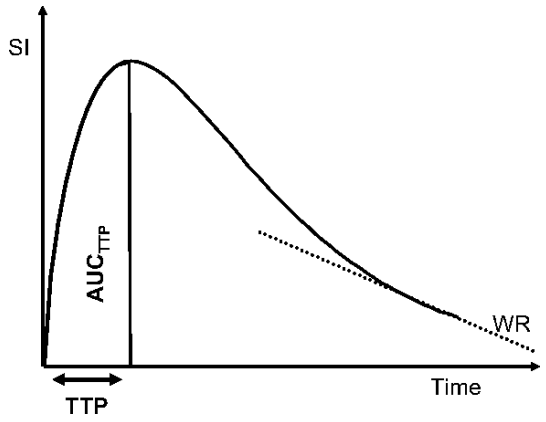

Fig. 2. Example of some features extracted from time-series (TTP, AUC_{TTP}, WR)

A binary Support Vector Machine (SVM) [11] classifier is used to distinguish among the several tumoral tissue classes. SVM constructs a maximal margin hyperplane in a high dimensional feature space, by mapping the original features through a kernel function. Since the Radial Basis Function (RBF) kernel has been used, two parameters C and γ need to be estimated. As previously suggested [12], data are properly normalized and parameters are estimated by combining grid search with leave-one-out cross-validation [1]. In order to extend the SVM to a multi-class framework, the one-against-all approach is carried out [1]. In our framework, such learning-by-example approach is introduced to better generalize the results. In fact, the SVM is able to automatically detect the most discriminative characteristics of the manually identified regions therefore allowing also the classification of new subjects.

The effect of the previously selected features in the classification have been assessed by comparing the results obtained by using (i) only two ($PEAK$ and TTP) features, (ii) all the five features and (iii) directly the raw n-dimensional time-series. The accuracy of the training phase of the SVM has been 89.1%, 95.4% and 99.8% using two features, five features and raw signals, respectively. This comparison allows a better identification of the most discriminative features by possible introducing a model selection phase.

Finally, in each tumour, the percentage volumes covered by each of the seven classes have been calculated to evaluate the time-dependent changes in control and treated tumours. The values obtained have been averaged over the experimental groups and statistically compared by paired t-test.

4 Results

The rate of tumour growth is strongly affected by the treatment; in fact average tumour volume, as determined by MR images, increased from $575 \pm 104\ mm^3$ to

1821±191 mm^3 in the control group and from 553±187 mm^3 to 788±227 mm^3 in the treated group. Table 1 summarizes the results of quantitative analysis in the treated and control groups. For each animal, the percentage volume attributed by the SVM classifier to each of the seven classes of signal intensity (S.I.) is reported before treatment (time point T_0) and after treatment (time point T_1).

		A		B		C		D		E		F		G	
		T_0	T_1	T_0	T_1	T_0	T_1	T_0	T_1	T_0	T_1	T_0	T_1	T_0	T_1
rawdata	Control	0,1	0,3	37,0	32,2	0,3	13,5	0,1	2,1	0,7	32,6	60,7	13,8	1,0	5,5
		1,7	1,4	12,4	22,5	4,6	5,7	2,6	2,5	8,2	9,2	68,3	56,2	2,3	2,5
		6,0	11,4	12,8	20,4	0,1	8,7	1,6	2,3	1,2	18,4	74,2	32,8	4,1	6,0
		4,3	7,1	4,9	16,0	0,6	4,6	1,7	2,7	3,8	23,7	83,6	38,3	1,2	7,6
		5,1	7,3	18,4	12,1	0,5	13,6	0,8	4,4	2,1	15,1	69,5	41,4	3,6	5,9
	Treated	14,3	9,0	13,1	12,6	1,5	4,4	4,9	3,0	4,5	9,4	58,7	55,6	3,1	6,0
		1,2	4,8	28,6	39,9	0,6	4,2	0,7	1,6	3,4	12,0	60,0	34,1	5,5	3,5
		3,4	13,5	34,1	19,1	0,3	1,5	3,3	3,9	3,4	10,6	50,0	43,4	5,5	8,0
		12,1	5,2	8,4	26,3	0,2	2,4	2,4	1,1	1,4	4,0	73,4	56,6	2,2	4,4
		5,0	11,2	21,0	23,2	4,8	4,3	6,7	8,0	8,6	13,6	47,0	30,0	6,8	9,7
		2,3	4,6	24,9	10,0	4,2	4,2	2,1	2,1	8,0	7,3	53,7	68,7	4,7	3,1
2 features	Control	0,1	0,4	32,4	23,7	3,3	22,7	0,1	1,2	3,3	27,1	58,8	18,3	2,0	6,7
		3,3	1,8	13,2	20,9	7,5	6,8	2,0	1,4	6,3	11,3	63,4	53,7	4,3	4,1
		4,4	10,0	7,3	17,2	0,4	8,6	1,2	2,0	2,9	18,3	77,6	36,4	6,2	7,4
		8,3	8,2	7,7	15,3	1,6	9,1	2,8	2,0	2,9	19,4	74,2	37,2	2,5	8,9
		5,1	7,6	14,9	9,2	1,9	16,7	1,1	4,0	5,6	15,5	64,8	40,9	6,6	6,2
	Treated	18,0	12,0	10,9	11,3	2,1	4,9	4,0	2,9	4,2	11,1	53,9	50,5	6,9	7,3
		1,3	4,5	19,5	29,8	2,7	5,5	0,5	1,0	10,0	11,7	58,0	40,9	8,1	6,6
		2,9	16,8	24,2	20,7	0,7	3,7	3,2	3,9	4,1	12,5	56,8	31,3	8,2	11,1
		15,7	4,3	11,7	16,7	0,3	8,6	2,9	1,0	2,1	9,0	63,6	55,0	3,6	5,4
		5,2	13,3	16,4	20,0	5,1	7,8	5,6	9,2	7,4	16,3	49,7	19,5	10,5	13,9
		2,5	7,1	21,1	10,4	4,4	8,8	1,6	2,7	8,2	9,8	56,3	56,4	5,9	4,8

Table 1. Percentage volume attributed by SVM classification algorithm to each of the seven classes `A-G` in each subject at time T_0 and at time T_1. Results relative to classification performed on rawdata and two features (TTP and $PEAK$) are shown.

Data reported in Table 1, averaged over the different experimental groups, are shown in Figure 3A (relative to the classification obtained by using raw data). In the control group there is a significant ($p < 0.05$) increase of the percentage volume covered by the classes `C` and `E` (i.e., the less enhancing portions of the tumours). Concomitantly, a significant ($p < 0.01$) decrease of the class `F` is observed. An increase in the scarcely enhanced tissue (mainly necrotic tissue) is typically observed during fast tumour growth. The increase of this tissue is less pronounced in treated tumours as expected from their reduced rate of growth. The percentage volume attributed to `A` and `D` classes (wash-out regions that correspond to well vascularized tissue) is not significantly affected by treatment (or normal tumour growth) in agreement with the fact that the biological target of

the herein investigated therapeutic treatment is represented by tumour cells and not by vasculature. Figure 3B shows percentage volumes of the different classes, averaged over the whole experimental group, relative to the classification obtained by using 2 features. Qualitatively, the alterations in percentage volumes of the different classes between time T_0 and T_1 are in agreement with those reported in Figure 3A, although there are some differences in their statistical significance. In selected animals standard histological and *CD31-immunohistochemical* examinations have been performed post-mortem according to [2]. These examinations qualitatively confirm the main findings of the present study.

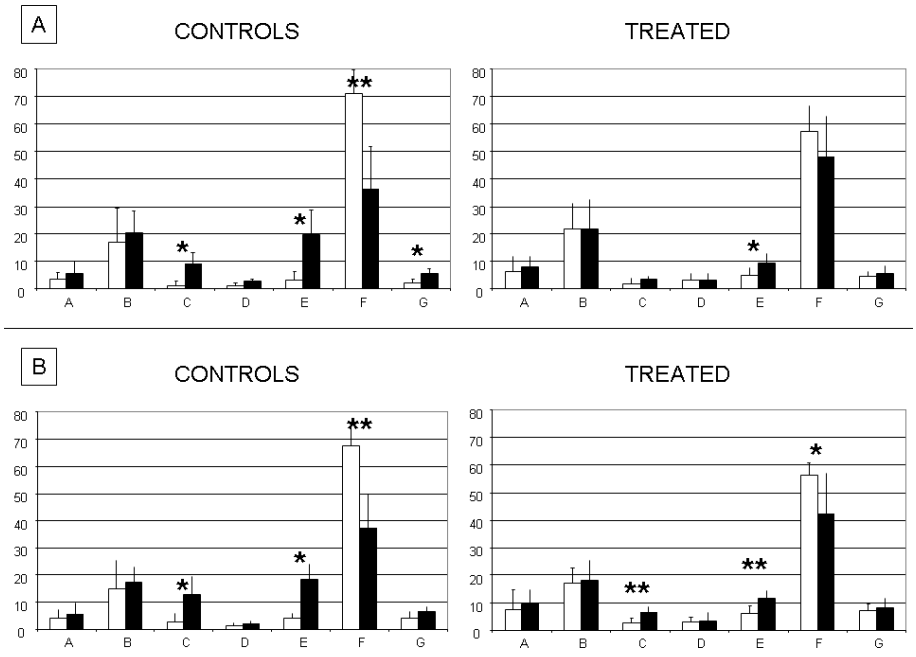

Fig. 3. Percentage volume (+ SD) attributed by the SVM to each of the seven classes `A-G` averaged over the different experimental groups (control and treated). White bars represent values at time T_0, black bars at time T_1. Data reported in (A) are relative to the classification obtained by using rawdata; data reported in (B) are relative to the classification obtained by using 2 features ($PEAK$ and TTP). Asterisks indicate t-test significance at a 0.05 (*) and 0.01 (**) level comparing T_0 vs T_1.

The differences between percentage volumes of a given class obtained by using raw data or two features (Table 1) are always less than 6% of the total volume. Comparable results (data not shown) are observed by using all the five defined features. These findings suggest that the identified features are able to summarize correctly the discriminative characteristic of the original DCE-MRI signals

wrt the addressed classification problem. The stability of the method with regard to the number of classes has not been tested at this stage.

Figure 4 shows segmentation of tumour images obtained with SVM in two representative animals (vehicle and drug treated) before and after the treatment. The substantial increase in the necrotic portion of the control tumour, typical of fast growing tumours, can be visually appreciated.

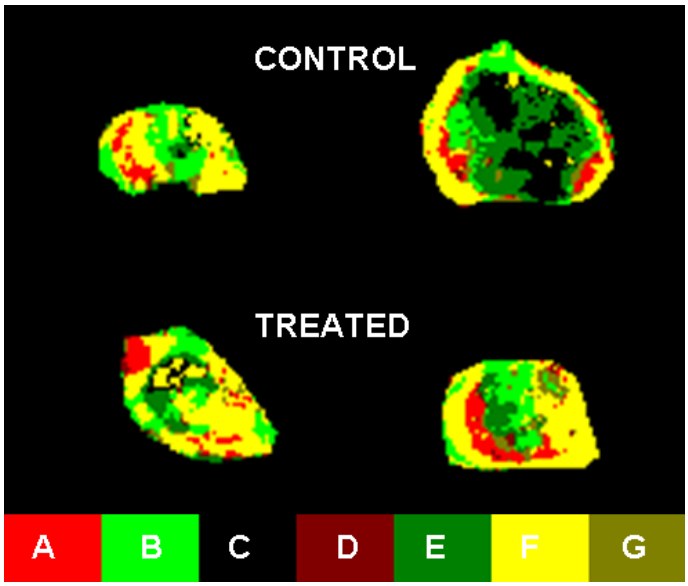

Fig. 4. Segmentation of tumour images in representative control and treated tumours at time T_0 (LEFT) and at time T_1 (RIGHT). The colorbar shows the colors used to identify the segmented classes.

In order to evaluate the effectiveness of the proposed method, we compared the regions obtained by SVM to those obtained by the standard k-means clustering algorithm (here $k = 7$). Figure 5 shows representative results obtained in two animals at time T_1 when using both algorithms on raw time-series. Each curve represents the time dependence of mean signal intensity over the extracted clusters. Both algorithms detect the necrotic areas (scarcely enhanced tissue), however whilst SVM is able to distinguish between wash-out and accumulation regions, k-means depicts mainly regions with similar enhancement (see Figure 5 TOP). Moreover, also the meaning of the viable tumor areas is more clear when regions are detected with SVM. In fact, by observing Figure 5 (BOTTOM) is possible to infer the limited presence of highly vascular regions (i.e., classes `A` and `D`) being the viable area mainly characterized by the intermediate class `B`. Such considerations are not feasible from the k-means clustering. Nevertheless, with

SVM-based segmentation the identification of corresponding regions among different subjects is obtained by construction, as opposed to k-means clustering for which such identification is not trivial (and in general for standard unsupervised segmentation methods). Therefore, the use of a data-driven algorithm appears unable to highlight regions with stable aspects and medical meaning, which can be only detected by a learning-by-example algorithm, such as SVM.

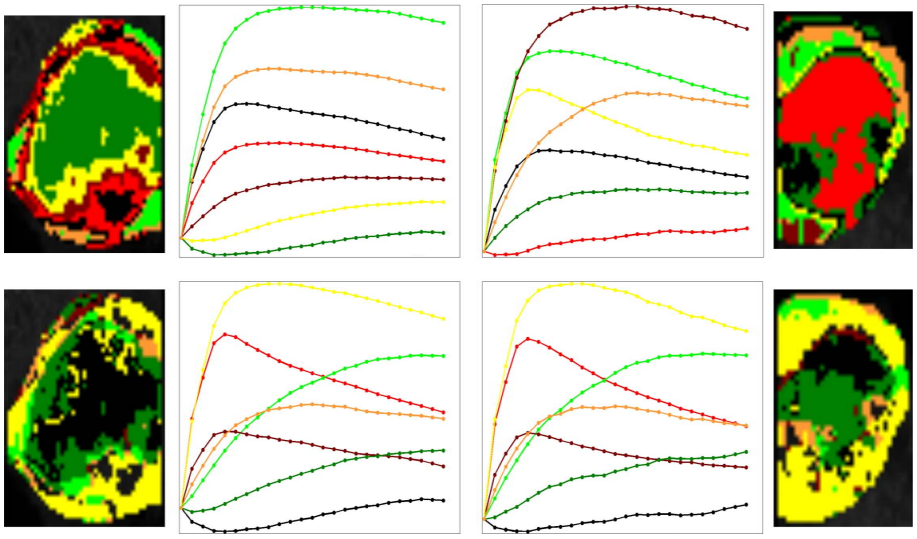

Fig. 5. Clustering results obtained with k-means (TOP) and SVM (BOTTOM) in two representative animals (time T_1): one control (LEFT) and one treated (RIGHT). The time-dependence of mean signal intensity for the extracted clusters is reported. Tumoral regions detected with our approach satisfy better the expected properties and the mean signal shapes are coherent with the taxonomy previously described.

5 Conclusions

In this paper we emphasize the use of a machine learning technique as a mean to produce automatic and meaningful segmentation results in the quantitative evaluation of DCE-MRI data. Specifically we have applied such technique in the analysis of DCE-MRI data to assess the effect of treatment with an experimental anticancer therapy. The SVM has been trained to detect biologically meaningful tumour regions of contrast agent accumulation and wash-out, as well as regions with negligible enhancement, attributable to necrotic tissue. The proposed approach permits the computation of percentage tumour volumes of above defined regions and to follow their modifications during the treatment with an experimental drug. The proposed comprensive experimental section have evidenced

the significative increase of necrotic volume on untreated subjects as confirmed by histological validation. Our results suggest that this approach can be useful in the analysis of heterogeneous tumour tissues and of their response to therapies.

References

1. Duda, R., Hart, P., Stork, D.: Pattern Classification. second edn. John Wiley and Sons (2001)
2. Marzola, P., Degrassi, A., Calderan, L., Farace, P., Crescimanno, C., Nicolato, E., Giusti, A., Pesenti, E., Terron, A., Sbarbati, A., Abrams, T., Murray, L., Osculati, F.: In vivo assessment of antiangiogenic activity of su6668 in an experimental colon carcinoma model. Clin. Cancer Res. **2**(10) (2004) 739–50
3. Castellani, U., Cristani, M., Combi, C., Murino, V., Sbarbati, A., Marzola, P.: Visual MRI: Merging information visualization and non-parametric clustering techniques for mri dataset analysis. Artificial Intelligence in Medicine **44**(3) (2008) 171–282
4. Lavinia, C., de Jongea, M., Van de Sandeb, M., Takb, P., Nederveena, A.J., Maas, M.: Pixel-by-pixel analysis of DCE MRI curve patterns and an illustration of its application to the imaging of the musculoskeletal system. Magnetic Resonance Imaging **25** (2007) 604–612
5. Stoutjesdijk, M.J., Veltman, J., Huisman, M., Karssemeijer, N., Barents, J., et al.: Automatic analysis of contrast enhancent in breast MRI lesions using Mean Shift clustering for roi selection. Journal of Magnetic Resonance Imaging **26** (2007) 606–614
6. Twellmann, T., Saalbach, A., Muller, C., Nattkemper, T.W., Wismuller, A.: Detection of suspicious lesions in dynamic contrast enhanced mri data. In: Engineering in Medicine and Biology Society. (2004) 454–457
7. Comaniciu, D., Meer, P.: Mean shift: A robust approach toward feature space analysis. IEEE Trans. Pattern Anal. Mach. Intell. **24**(5) (2002) 603–619
8. Castellani, U., Cristani, M., Daducci, A., Farace, P., Marzola, P., Murino, V., Sbarbati, A.: DCE-MRI data analysis for cancer area classification. Methods of information in medicine (To appear)
9. Marzola, P., Ramponi, S., Nicolato, E., Lovati, E., Sandri, M., Calderan, L., Crescimanno, C., Merigo, F., Sbarbati, A., Grotti, A., Vultaggio, S., Cavagna, F., Russo, V.L., Osculati, F.: Effect of tamoxifen in an experimental model of breast tumor studied by dynamic contrast-enhanced magnetic resonance imaging and different contrast agents. Investigative radiology **40**(7) (2005) 421–429
10. Marzola, P., Degrassi, A., Calderan, L., Farace, P., Nicolato, E., Crescimanno, C., Sandri, M., Giusti, A., Pesenti, E., Terron, A., Sbarbati, A., Osculati, F.: Early antiangiogenic activity of SU11248 evaluated in vivo by dynamic contrast-enhanced magnetic resonance imaging in an experimental model of colon carcinoma. Clin. Cancer Res. **11** (Aug 2005) 5827–5832
11. Burges, C.: A tutorial on support vector machine for pattern recognition. Data Mining and Knowledge Discovery **2** (1998) 121–167
12. Chang, C.C., Lin, C.J.: LIBSVM: a library for support vector machines. (2001)